Annuaire de l'Universite de Sofia "St. Kliment Ohridski", Faculte de Physique, 101, 2008

STRUCTURAL, MAGNETIC AND TRANSPORT PROPERTIES OF $RE_{1-X}M_XMNO_3$ MATERIALS, CERAMICS AND SEMIMAGNETIC SEMICONDUCTORS M_{1-X} RE_XMNTE INDUCED BY MN IONS AND OXIDES

ZAHARI ZLATANOV

Department of General Physics

Захари Златанов. СТРУКТУРНИ, МАГНИТНИ И ТРАНСПОРТНИ СВОЙСТВА НА $RE_{1-x}M_xMnO_3$ МАТЕРИАЛИ, КЕРАМИКИ И ПОЛУМАГНИТНИ ПОЛУПРОВОДНИЦИ M_{1-x} RE_xMnTe, ПОВЛИЯНИ ОТ МАНГАНОВИ ЙОНИ И КИСЛОРОД

В тази статия са представени някои от последните изследвания в една широка област от материали $RE_{1-x}M_xMnO_3$, класифицирани като манганови оксиди, керамики и полумагнитни полупроводници M_{1-x} RE_xMnTe, съдържащи Mn-йони и окиси. Голяма част от последните работи се отнасят до мангановите оксиди със смесена валентност, показващи преход метал–изолатор, съпроводен с т. нар. ефект на свръх голямо магнитосъпротивление, което се свързва с преход от феро- към парамагнитна фаза. Типичен представител на такива материали е съединението от тип перовските $LaMnO_3$. Близо до температурата на фазовия преход, която може да превишава стайната температура при някои състави, се наблюдава голямо магнитосъпротивление, като това дава възможност за прилагането на тези материали при магнитнитни записи. Такова свръхголямо магнитосъпротивление също така се наблюдава и в друга, доста различаваща се от типа манган–перовските материали, група съединения – Cr-халкогенидни спинели. В случаят на легираните полумагнитни полупроводници $A^{IV}B^{VI}$ (напр. $Pb_{1-x}Mn_xTe$, $Pb_{1-x}Gd_xTe$) след отгряване при високи температури (над 650 K) на въздух, тези материали е възможно да претърпят промяна на някои структурни и магнитни свойства. След отгряването и окисляването тези свойства, като тип структура и съпротивление наподобяват тези на RE(M=)MnO_3 и на някои керамики. Възможно е полумагнитните полупроводници, съдържащи летливия елемент Te, да показват преход от rock-salt структура в perovskite и заместване на част от телуровте атоми с тези на кислорода в подрешетката на Te. Такъв преход може да се наблюдава за материалите PbMnTe и PbGdMnTe (NaCl-perovskite) във фазите MnTe и GdTe. Или в случай на редкоземни полумагнитни полупроводници с MnTe-фаза това явление ще се наблюдава при високи температури в присътвие на кислород.

Zahari Zlatanov. STRUCTURAL, MAGNETICT AND TRANSPORT PROPERTIES OF $RE_{1-x}M_xMnO_3$ MATERIALS, CERAMICS AND SEMIMAGNETIC SEMICONDUCTORS M_{1-x} RE_xMnTe INDUCED BY Mn IONS AND OXIDES

In this article are review recent works falling under the broad classification of manganese oxides $RE_{1-x}M_xMnO_3$, ceramics and semimagnetic semiconductors M_{1-x} RE_xMnTe induced by Mn ions and oxides. Large part of the recent studies has been devoted to the mixed valence manganese oxides exhibiting a metal insulator transition accompanied by so called colossal magnetoresistance (CMR) effects, which is magnetoresistance associated with a ferromagnetic-to-paramagnetic phase transition. The prototypical CMR compound is derived from the parent compound, perovskite $LaMnO_3$. Near the phase transition temperature, which can exceed room temperature in some compositions, large magnetoresistance is observed and it is possible application in magnetic recording has revived interest in these materials. Large magnetoresistance is also seen in other systems namely Cr chalcogenide spinels, compounds which differ greatly from the manganite perovskites In the case of the doped $A^{IV}B^{VI}$ semimagnetic semiciductors (SMSC) (example: $Pb_{1-x}Mn_XTe$, $Pb_{1-x}Gd_xTe$) was looked, after hot annealing on air (at temperature over 650 K) change of some properties-structural and magnetic. They were transformred to similar of the RE(M=)MnO_3 materials and some ceramics (structure–perovskite, resistivity-CMR). It is possible that SmSc shows the temperature induced transition from rock-salt (collinear) to perovskite (spiral magnetic) structure. associated with oxide atoms ordering in the Te sublattice. Such a transition could observed for PbMnTe and PbGdMnTe (NaCl-perovskite) in the GdTe and MnTe-ordered phase**.** Or of the case of rare-earth SmSc with MnTe phase this phenomenon will be observing at relatively high temperatures.

***Keiwords*:** semiconductors, structure, magnetic, transport properties
PACS number: 61.72-Y

1. INTRODUCTION

More recently, it has become recognized that some materials, specifically transition metal oxides, possess large room–temperature magnetoresistivity associated with a paramagnetic–ferromagnetic phase transition. An enormous amount of work was devoted to the mixed-valence oxides, mainly to the manganites $RE_{1-x}M_xMnO_3$ (RE = rare-earth, M = Ca, Sr, Ba, Pb) with three–dimensional perovskite-type structure. The investigations were carried out on polycrystalline sintesed samples, single crystals, and thin films. The compounds which have been the focus of the majority of studies are the manganite perovskites $RE_{1-x}D_xMnO_3$, where RE is a trivalent lanthanide cation (e.g. La) and D is a divalent, e.g. alkaline-earth (e.g. Ca, Sr, Ba), cation. The experiments were then extended to other oxides such as the layered manganites (for example: $La_{2-2x}Sr_{1+2x}Mn_2O_7$ [1] and Sr_2MoFeO_6 [2]).

The most important features of the physics of these oxides to avaluate their potential applications. Special attention is devoted to epitaxial thin films.

The growth techniques and the changes in their properties with respect to bulk oxides due to interfaces and epitaxial strains are reviewed. These oxides have a rich and complex physics related to the large importance of electron–lattice and electron–electron interactions. Their structural, magnetic transport properties are intrically related. In addition, the negative magnetoresistancects and the occurrence of metallic phases with a fully spin-polarized conduction band are promising for are promising for potential applications.

A large part of the recent studies has been devoted to the mixed-valence manganese oxides exhibiting a metal insulator transition accompanied by so called colossal magnetoresistance (CMR) effects [3–7]. These recent experimental works falling under the broad classification of colosall magnetoresistance. This magnetoresistance associated with a ferromagnetic–to–paramagnetic phase transition. The prototypical RE(M)MnO compound is derived from the parent compound, perovskite $LaMnO_3$. When hole doped at a concentration of 20–40% holes / Mn-ion, for instance by metal ion (Ca or Sr) substitution for rare-earth atom (RE = La), the material displays a transition from a high-temperature paramagnetic insulator to a low-ferromagnetic metal. Near the phase transition temperature, which can exceed room temperature in some compositions, large magnetoresistance is observed and its possible application in magnetic recording has revived interest in these materials (Fig. 1). Large magnetoresistance is also seen in other systemsm namely Cr-chalcogenide spinels, compounds which differ greatly from the manganite perovskites.

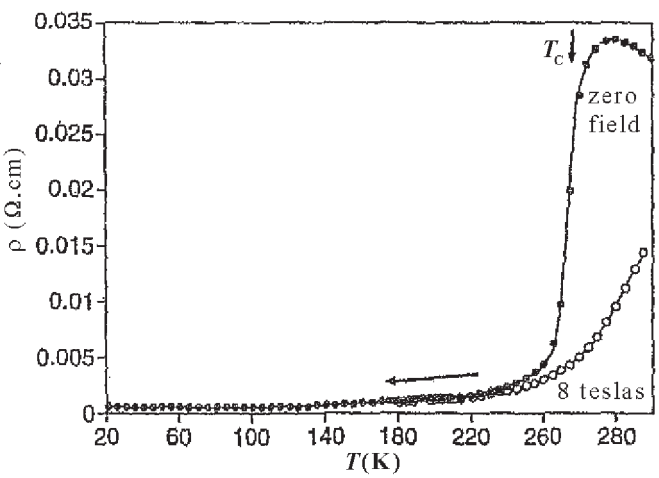

Fig.1. Resistivity in zero field and in a 8 *T* applied fieldd versus temperature, of a single crystal of $La_{1-x}(M = metal)_xMnO_3$ (for example $La_{0.825}\ Sr_{0.175}\ Mn0_3$). The array indicates the Curie temperature, T_C (A. Anane et. al.[44])

The physical properties of these manganites have been extensively described and discussed in review papers [8, 9]. In same works Zener proposed a mechanism he called "double exchange" (DE) to explain the simultaneous occurrence of ferromagnetism and metallicity. The both as a function of x and T, found by Jonker and van Santen [10**]**.The FM state is observed only for finite D concentration where electronic transport is via holes arising from charge exchange between ion (Ca^{2+} for example) and Mn. In agreement with this simple single-ion model, the manganites with strong distortion of the oxygen octahedron have a large magnetic anisotropy.

It has been recently predicted from computational studies of realistic models that an electronic phase separation can occur in manganites in a certain range of doping [11]. In particular, at low doping level and at low temperature, a phase separation between hole-poor AF regions and hole-rich F regions is energetically more favourable than the homogenous canted AF phase. The energy of the charge carriers is minimal for F ordering. With a density insufficient for establishing the F ordering in the entire sample, the carriers concentrate into droplets or stripes which become ferromagnetic inside the insulating AF matrix. Such a phase separation was predicted earlier for degenerate magnetic semiconductors and conjectured for manganites [12]. Experimental observation of electronic phase separation in manganites is not as straightforward. Local probes such as neutron scattering and nuclear magnetic resonance (NMR) are needed and the data interpretation is rarely unambiguous [13].

Other class of materials with cubic space group are PFT complex perovskite (for example: $PbFe_{0.5}Ta_{0.5}O_3$). PFT were first prepared as a ceramic by Smolenski *et. al.* [14] in 1959. They are presents some unsolved crystallographic problems. These compounds belongs to the wide family of lead-based oxides with general formula $PbB'_{0.5}B''_{0.5}O_3$, in which two cationic species, in a 1:1 ratio, occupy the B-site lattice of the perovskite structure ABO_3. These materials have been and still are extensively studied for their interesting ferroic behaviour. They generally undergo a sequence of temperature-induced phase transitions, which can either be purely structural (ferroelastic) or lead to ferro/antiferroelectric, ferro/antiferromagnetic final states. Phase transitions in perovskite-type compounds consist in small modifications of a high-symmetry, ideally undistorted structure—the one stable at the highest temperatures —which is called the parent phase or prototype.

The sequence of phases in PFT one can find in Landolt–Bornstein, i.e. the one determined for ceramic samples, is quite simple: at room temperature the geometry of the X-ray powder diffraction pattern was reported to be cubic space group $Pm\bar{3}m$. For PbFeTaO a lattice parameter of about 4Å, corresponding to Fe^{3+} and Ta^{5+} statistically distributed over B-sites.

Goodenough *et. al.* have reported that ternary oxides $La(Mn_{0.5}Me_{0.5})O_3$ (Me = Ni, Co) with a cubic perovskite structure are ferromagnets [15]. Blasse has suggested the ferromagnetism to be governed by the positive superexchange interaction between metal ion (Co^{2+}) and Mn^{4+} ions via oxygen [16]. The metal ions and Mn^{4+} ions in samples prepared at low temperature are crystallographically ordered to a considerable extent, making up the rock -salt type lattice [16]. This model was supported by the results of NMR measurements[17, 18]. Recently the $R(Mn_{0.5}Co_{0.5})O_3$ (R = Nd, Sm, Eu, Gd, Tb, Dy, Y) compounds have been obtained using a conventional ceramic method. These compounds were found to be ferromagnets with relatively high Curie temperature and spontaneous magnetization.

A considerable amount of works has been done on the study of the class of materials known as semimagnetic semiconductors. Indeed, the subject has been introduced by M. Rodot and co–workers who investigated the exchange interactions of manganese ions (Mn^{2+}) diluted in II–VI compounds [19–21].

The host matrix is either SnTe, GeTe, or PbTe. Mn^{2+} is the most convenient impurity, because of its electronic configuration $3d^5$ with zero orbital momentum (S state). Then, there is no spin–orbit interaction giving rise to anisotropy effects, and the experimental results are interpreted more easily. The magnetic properties of $Ge_{1-x}Mn_xTe$ and $Sn_{1-x}Mn_xTe$ are well understood.

The ferromagneting ordering of these alloys is due to the Ruderman–Kittel–Kasuya–Yosida (RKKY) interaction mediated by the 10^{20}–10^{21} cm^{-3} free carriers (holes). The carrier concentrations in $Pb_{1-x}Mn_xTe$ however, are much smaller, and so is the RKKY interaction, so that the magnetic behavior of this material is much more complex [22]. The Currie–Weiss temperature is negative and small for both clustered and single spins, reflecting a weak antiferromagnetic interaction.

Gadolinium-doped PbTe and SnTe semiconductors have been studied recently by several groups [23–28]. These systems are examples of narrow–gap dilute magnetic semiconductors. The interest in this class of compounds centres on the effect caused by the interactions between the carriers and the magnetic moment of the dopands. While the 3d dopand Mn has been extensively studied, less is known about the 4f dopand Gd. For Gd in PbTe and SnTe, Shubnikov–de Haas oscillations, as well as very high mobilities, are reported in [23].

Measurements of electron paramagnetic resonance (EPR) and of susceptibility have been performed on $Pb_{0.995}Gd_{0.005}Te$ crystals. The EPR spectra consist of two components, one showing the fine structure of Gd^{3+} ions in a cubic environment. The Curie–Weiss temperature θ in these alloys is small and negative, reflecting a weak antiferromagnetic exchange interaction between the Gd ions, similar to that of Mn in PbTe [29].

Here are presented the study and the results of magnetic and transport properties of other class semimagnetic semiconductors M(MnRE)SnTe ($Pb_{1-x-y-z}Mn_xSn_yEu_zTe$). AC magnetic susceptibility measurements as well as transport characterization were performed. The obtained results indicate that the presence of two types of magnetic ions influences the magnetic properties of the investigated IV-VI semimagnetic semiconductor. Qualitative analysis and possible mechanisms of the substantial dependence of the Curie temperature on the Eu content are presented. The most likely reason of the observed Curie temperature behaviour is a strong dependence of the location of a heavy mass Σ band upon the alloy composition. Theoretical calculations in frame of simple models confirm this point.

2. EXPERIMENTS, DATA AND DISCUSSION

The manganese oxides of general formula $RE_{1-x}M_xMnO_3$ (RE = rare-earth, M = Ca, Sr, Ba, Pb) have remarkable interrelated structural, magnetic and transport properties induced by the mixed valence (3+–4+) of the Mn ions. In particular they exhibit very large negative magnetoresistance (called colossal magnetoresistance–CMR), in the vicinity of metal–insulator transition for certain compositions. Some materials, specifically 3d-transition metal oxides, possess large room-temperature magnetoresistivity associated with a paramagnetic–ferromagnetic phase transition.

The compounds which have been the focus of the majority of studies are the manganite perovskites $T_{1-x}D_xMnO_3$ where T is a trivalent lanthanide cation (e.g. La) and D is a divalent, e.g. alkaline-earth (Ca, Sr, Ba), cation. The materials $REMMn0_3$ ($La_{1-x}M_xMnO_3$) were studied in the fifties, both experimentally [30] and theoretically [31,32]. The experiments performed on polycrystalline samples mixed-valence perovskites showed antiferromagnetic (AF) insulating behaviour at low and high x values and ferromagnetic (F) metallic behaviour in a certain range of concentrations centred around $x \approx 1/3$. This striking behaviour was early explained by the theory of double-exchange (DE) [31,32].

For the end members of the dilution series, $LaMnO_3$ and $CaMnO_3$, the ground state is antiferromagnetic (AF), as expected for spins interacting via the superexchange interaction when the metal–oxygen–metal bond angle is close to 180°. In a certain range of doping, $x \sim 0.2–0.4$, the ground state is ferromagnetic (FM), and the paramagnetic-to-ferromagnetic transition is accompanied by a sharp drop in resistivity $\rho(T)$. This phenomenon has been known to exist since 1950.

Recently, interest in these materials has been renewed by the realization that:

(1) the magnetoresistance (MR) associated with this correalation between magnetization (*M*) and resistivity (ρ) can be very large, and (2**)** the basic interaction responsible for the ρ – *M* correlation, the double-exchange (DE) interaction [33] between heterovalent (Mn^{3+}, Mn^{4+}) neighbours, is by itself not sufficient to explain this MR [34]. Both the large resistance and the associated MR are now thought to be related to the formation of small lattice polarons in the paramagnetic state. The large MR resulting from the transition has been called "colossal magnetoresistance" [35], mainly to distinguish it as a phenomenon distinct from GMR. In addition to the renewed interest in the FM state, much attention has been given to another type of collective state, charge order (CO), typically observed for $x > 0.3$. At these doping levels CO can compete with the FM ground state, leading to complex electronic phase behaviour as chemical formula is varied [36,37].

In some articles were collected experimental results necessary for an empirical understanding of the various ground states in the manganite perovskites and present a comparison between the different compounds exhibiting negative magnetoresistance. The understanding developed to explain CMR in the manganite perovskites does not carry over easily to two other CMR compound families–the pyrochlores, e.g. $Tl_2Mn_2O_7$ [38].

2.1 MATERIALS. OBTAINING AND STRUCTURE

Recently was synthesized and characterized a series of compounds with the general formula $T_{1-x}D_xMnO_3$ where T is trivalent ion and D is a divalent ion. These compounds form in the structure of perovskite. In this structure, the T, D and M ions form interpenetrating simple cubic sublattices with O at the cube faces and edges.

The crystal structure and lattice parameters obtained by neutron powder diffraction are given for a series of solid solutions (for example: $La_{1-x}Ba_xMn_{1-y}Ti_yO_3$ [39]). All the compounds studied, which include the end member $LaMnO_3$, are isostructural, crystallizing in the orthorhombic *Pnma* structure at room temperature.

The end member $LaMnO_3$ is very distorted: the octahedra are elongated and tilted. Though tilting distortions are not unusual for perovskites simply on the basis of steric conditions, its magnitude in $LaMnO_3$ and the presence of elongation are thought to be the result of a Jahn–Teller local distortion [40].

Jirak *et. al.* have shown that for $Pr_{1-x}Ca_xMnO_3$, there exists a phase tran-

sition between a high–temperature pseudo–cubic phase and an orthorhombic phase. This structural transition temperature exceeds 900 K for $x = 0$ and decreases to room temperature at around $x = 0.3$, the doping level where the FM state appears, suggesting a strong magneto–elastic coupling. The structure of compounds exhibiting CMR is usually orthorhombic but, for doping levels near the T = 0 metal–insulator boundary, the symmetry can be modified by application of magnetic field.

Crystallographic structure

The structure of the $RE_{1-x}M_xMnO_3$ oxides is close to that of the cubic perovskite. The large sized RE trivalent ions and M divalent ions occupy the A–site with 12–fold oxygen coordination.The smaller Mn ions in the mixed–valence state Mn^{3+}-Mn^{4+} are located at the centre of an oxygen octahedron, the B–site with 6–fold coordination. For the stoichiometric oxide, the proportions of Mn ions in the valence states 3+ and 4+ are respectively, $1– x$ and x.

The structure of the manganites is governed by the tolerance factor:

$$t = \frac{(r_A + r_o)}{2^{1/2}(r_B + r_o)}. \tag{1}$$

Generally, t (tolerance factor) differs appreciably from 1 and the manganites have, at least at low temperature, a lower rhombohedral symmetry or orthorhombic structure. This is illustrated by the orthorhombic structure of $LaMnO_3$, which is the parent compound of the most investigated manganites for potential application by partial substitution of La by Ca and Sr.

The early work of Jonker and van Santen established the range of possible solid solutions allowed by the Goldschmidt tolerance factor:

$$t = \frac{(r_D + r_o)}{\sqrt{2}(r_T + r_o)} \sim 1, \tag{2}$$

where r_D, r_T and r_o are the radii of the divalent, trivalent and oxygen ions respectively. The tolerance factor measures the deviation from perfect cubic structure ($t = 1$). The perovskite structure is stable for $0.89 < t < 1.02$, $t = 1$corresponding to the perfect cubic closely packed structure.

By using some mixtures, t can be varied, with the result that the perovskite structure is stable for $0.85 < t < 0.91$(T = La, Pr, and Nd and D = Ca, Sr, Ba, and Pb). At finite doping, charge balance is maintained by a fraction, x, of Mn ions assuming a tetravalent, Mn^{4+} (d^3), configuration in a random fashion

throughout the crystal, with the remainder in the Mn^{3+} (d^4) state. Presumably, D substitution is equivalent to hole doping, but thermopower and Hall effect disagree on the carrier sign in the paramagnetic state, suggesting that a simple band picture is not valid.

When Gd is substituted for Pb in PbTe in the NaCl structure, it is surrounded by 12 cation sites connected to it by a pair of bonds at right angles. In addition, six more cation sites are connected by a pair of collinear bonds. For a random distribution of 0.5 at % Gd, the ratio of pairs of Gd ions to single ions is, to a good approximation: $r:(1-r)$, where r = 18x0.005, i.e. 0.10 : 1 (3)

Doping level and A–site cation size

The physical properties of perovskite–type manganites are determined by two main parameters : the doping level, x = Mn^{4+} / (Mn^{3+} +Mn^{4+}), and the average size of the cation A, (r_A). A third relevant parameter is the degree of disorder at site A, defined by $\sigma^2 = (r_A^2) - (r_A)^2$. An enormous number of experimental studies has been performed to quantify these effects. Roughly speaking the ferromagnetic DE is maximum around x = 1/3 and for (r_A) ~ 1.24 Å. The reduction of (r_A) from this optimum value leads to an increasing distortion of the crystallographic structure. The resulting reduction of the Mn–O–Mn angle from 180° to a smaller value weakens the F DE and increases the tendency to localize the charge carriers. This effect of (r_A), which is drastic on the resistivity [41], is exemplified by the phase diagram for x = 0.3 [42]. Similar detailed studies for x = 0.5 have been already published [43].

A striking effect of the coupling between magnetism and the structure is observed when the temperature of structural transition, T_S, becomes close to T_C: TS is shifted by changing the degree of alignment of the Mn spins by an applied field [44, 45]. This can be qualitatively interpreted by a field induced delocalization of the charge carriers which stabilizes the less distorted of the two structures involved in the structural transition.

The most intriguing problem concerns the cubic room–temperature phase: it was found that crystals of PFT grown from PbO flux, which display the {100} cubic form, are actually composed of six pyramidal growth sectors uniaxial from the point of view of optical symmetry (Fig. 2). The value of the birefringence, due to a positive tetragonal indicatrix, is of the order of 10^{-4}. Sectors are disposed in such a way to give individual crystals with octahedral point symmetry (Fig. 3).

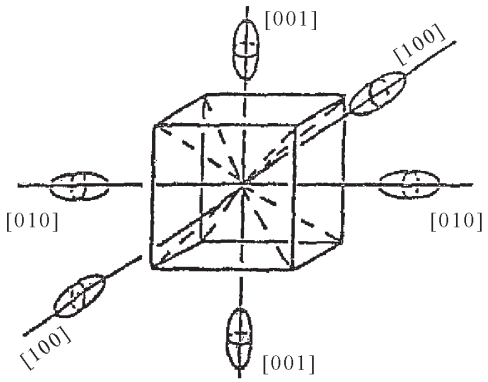

Fig.2. Orientatioanal states of the uniaxial indicatrix with respect to (100) growth sector

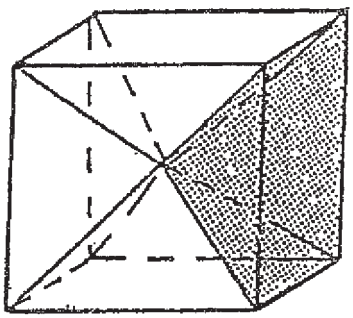

Fig.3. Optically tetragonal sectors disposed to give individuals with overall octahedral symmetry

Effect of Pb disorder in the prototype of PbB'0.5B"0.5O3 compounds

The cubic prototype of Pb–based 1 : 1 complex perovskites has some peculiar structural features which will be described in the following. The ideal structure is shown in (Fig. 4) for statistical disorder on site B; the ideal structure has symmetry $Pm\bar{3}m$ and a lattice parameter of about 4 Å; Pb is at the origin of the cell, B and B' share the central octahedral site and oxygen atoms are located at the centres of the faces of the cube. The structure was very well refined as cubic disordered, with disorder confined only at the Pb site. Most models represented in (Fig. 4) give comparable results, in which some of them are briefly compared.

The cubic disordered structure reflects the overall symmetry averaged over a large number of cells, each one of tetragonal symmetry if Pb is on (x00) positions (of Fig. 5). Correlations among such unit cells could explain the observed birefringence.

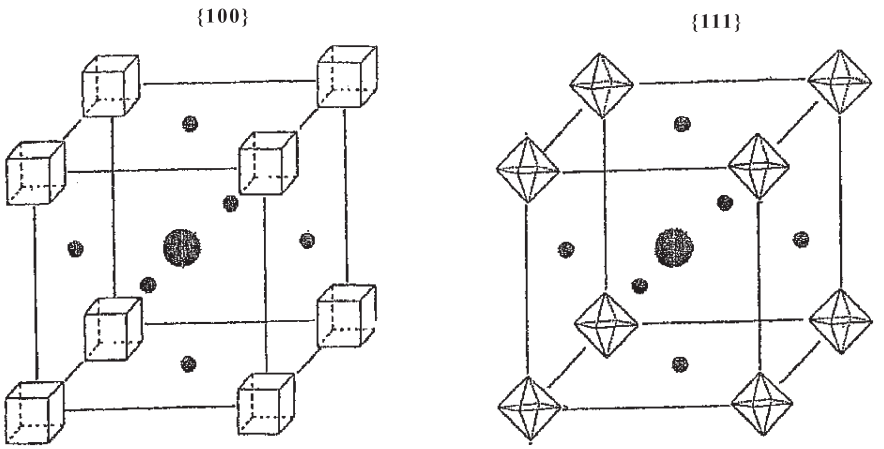

Fig.4. Representation of disordered $Pm\bar{3}m$ structures. In the disordered structure, Pb statistically occupies several equivalent positions (Wyckoff positions) around the origin of the cubic cell: a) tetragonal; b) rhombohedral

A good tetragonal model appeared to be the one shown in (Fig.5). The weak uniaxial anisotropy rises from planar disorder of Fe / Ta atoms, which are split on 4k positions in the plane perpendicular to the unique *c* axis.

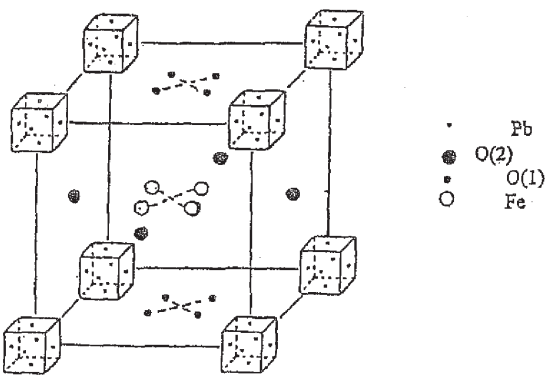

Fig.5. Tetragonal model here with proposed ($PbFe_{0.5}Ta_{0.5}O_3$)

The disorder of Pb in connection with the ferroic transitions

The disordered configuration of Pb has been shown to be the most interesting feature of the refined structure of PFT, whether tetragonal or cubic. This compound then increments the list of Pb-based complex perovskites with A-site positional disorder. Beside the general interest in disordered crystalline structures, the particular importance of this kind of disorder whether at site A or B – in perovskite-type ferroics resides in the fact that its presence seems to imply an order – disorder component even in those which were traditionally considered the most typical examples of displacive phase transitions. Positional disorder at site B has been discussed in the framework of the so – called eight–site model [32], according to which the sequence of distortive ferroelectric transitions in perovskites would be better regarded as a sequence of order – disorder processes taking place at the octahedral sites. The model, proposed for barium titanate, suggests that starting from the isotropic (i.e. cubic) situation in which the cation B has access to eight equivalent sites disposed symmetrically along $\{111\}_{cub}$ directions around the (1/2, 1/2, 1/2) Wyckoff position, the low – temperature phases (i.e. the tetragonal, then the orthorhombic and finally the rhombohedral ones), are obtained by constraining the B cation to occupy just four, then two and finally one of the eight previous sites.

The hypothesis can be formulated that an analogous model is valid for site A in all compounds which have Pb^{2+} as large cationic species. Stereochemical considerations suggest, in fact, that the ion Pb^{2+}, with its lone pair of electrons, would never be found at the origin of the cubic perovskite cell, as has been stressed for example in [46]. One way to retain the cubic symmetry would be the adoption of a split configuration. At least if the disorder of Pb is thermally activated, transitions towards more ordered, less symmetric phases can occur when the temperature is lowered.

2.2 MAGNETIC PROPERTIES

Magnetic anisotropy Exchange interactions

The magnetic properties of the manganites are governed by exchange interactions between the Mn ion spins. These interactions are relatively large between two Mn spins separated by an oxygen atom and are controlled by the overlap between the Mn *d*-orbitals and the O *p*-orbitals.

In the manganites with perovskite structure, the easy magnetization axis is determined by the magnetocrystalline anisotropy resulting from the combined effects of crystal field and spin – orbit coupling. For the sake of simplicity, here will consider the manganite composed of Mn^{3+} and Mn^{4+} ions with re-

spective proportions of $1 - x$ and x, and with a magnetic anisotropy that is the weighted sum of the single – ion anisotropies of Mn^{3+} and Mn^{4+}.

The Mn ion is surrounded by an octahedron of oxygen atoms, more or less axially distorted depending on x. The distortion is strong in Mn^{3+} rich manganites such as $LaMnO_3$ [47] due to the large Jahn–Teller effect of Mn^{3+} and it gradually decreases with increasing the concentration x in Mn^{4+}.

Generally, for Mn^{4+}–O–Mn^{4+}, the interaction is AF, whereas for Mn^{3+}–O–Mn^{3+} it may be ferro–or AF [32], such as in $LaMnO_3$ where both F and AF interactions coexist. The magnetic properties of $RE(Mn_{1-x}Co_x)O_3$ solid solutions are governed by magnetic interactions between different magnetic ions. The most important interactions are antiferromagnetic Mn^{3+}–O–Mn^{3+}, Co^{2+}–O–Co^{2+} and Mn^{4+}–O–Mn^{4+} and ferromagnetic Co^{2+}–O–Mn^{4+} and Mn^{3+}–O–Mn^{4+}. It was supposed that Co^{3+} ions have low – spin diamagnetic state and play a passive role in the superexchange interaction. Important to note that Mn^{3+}–O–Mn^{3+} magnetic interaction in a perovskite lattice becomes positive if the Mn – O – Mn angle is close to 180^o.

A peculiar and interesting case is that of Mn^{3+}–O–Mn^{4+}, for which the Mn ions can exchange their valence by a simultaneous jump of the e_g electron of Mn^{3+} on the O p-orbital and from the O p-orbital to the empty e_g orbital of Mn^{4+}. This mechanism of DE originally proposed by Zener [31] ensures a strong ferromagnetic-type interaction.

The crystal field experienced by the Mn ion is thus composed of two contributions: a large cubic contribution since the symmetry is predominantly cubic, and a smaller tetragonal contribution roughly proportional to the axial elongation of the oxygen octahedron.

Ferromagnetic metallic (FM) phases with high Curie temperature, T_C, are required for potential applications. In the first approximation, one can neglect the Mn^{3+} – M^{n3+} interaction since it is either F or AF depending of the orbital configuration and both F and AF interactions currently coexist in the same compound such as in $LaMnO_3$ Mixed valency can also be modified by varying the oxygen content. For $x \sim 0$ and 1, M ($T < 100$ K) was found to be small, indicating an antiferromagnetic (AF) ground state. At intermediate values of x, M rises and peaks with its Hund's-rule value at $x \sim 0.3$. In the work of van Santen and Jonker showed that at temperatures above the ferromagnetic Curie point, T_C, the resistivity behaves like a semiconductor, $d\rho / dT < 0$, but that below T_C, not only is there a sharp reduction in resistivity, but also a transition to metallic behaviour, $d\rho / dT > 0$. This behaviour is shown for $La_{1-x}Sr_xMnO_3$ and $La_{1-x}Ca_xMnO_3$ in (Fig. 6) and (Fig. 7).

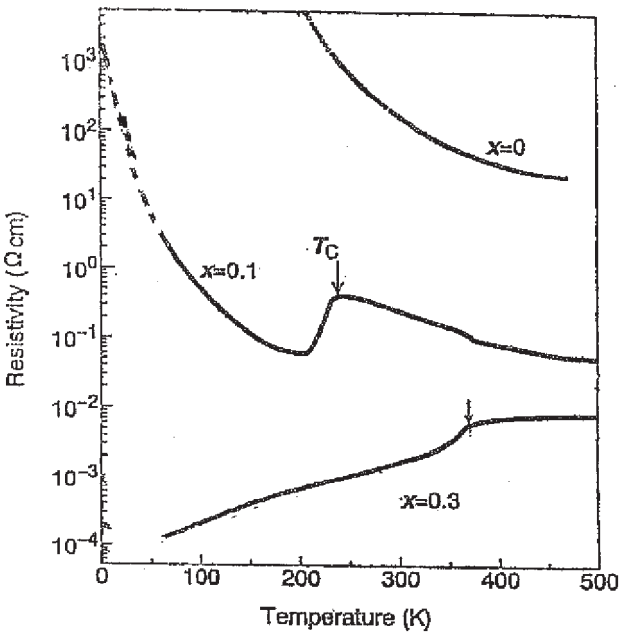

Fig.6. Resistivity against T for $La_{1-x}Sr_xMnO_3$ for various x values. The arrows denote the transition as determined by magnetization measurements

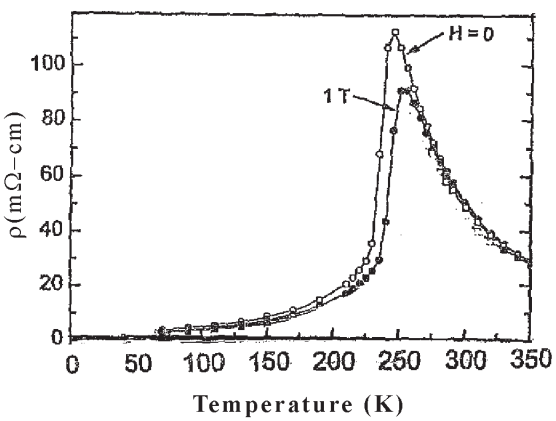

Fig.7. Resistivity against temperature

Magnetic ordering in perovskites containing manganese and cobalt

For better understanding of the magnetic properties of the perovskites containing manganese and cobalt ions in some studies were prepared RE $(Mn_{1-x}Co_x)O_3$ (R= Eu, Gd, Tb) solid solutions and have investigated their mag-

netic properties in a wide range of magnetic fields and temperatures. It has been found that some compounds (for example $EuMnO_3$ and $GdMnO_3$) are weak ferromagnets of Dzialoshinsky–Moriya type, whereas other materials ($TbMnO_3$) are antiferromagnets.

The substitution of manganese ions by metal ions (cobalt)ones leads to the appearance of different magnetic states: cluster-spin-glass-like ($0.1 < x < 0.3$), inhomogeneous ferromagnets with well defined Curie temperatures ($0.4 < x < 0.8$) and again a spin glass state ($x > 0.9$). Spontaneous magnetizations and Curie temperatures reach maxima for compounds with $x = 0.5$. External magnetic field induces a metamagnetic transition in RE $(Mn_{0.5}Co_{0.5})O_3$ (R = Gd, Tb, Y). The metamagnetic behaviour is interpreted taking into account the ionic ordering of Co^{2+} and Mn^{4+} ions and possible 3*d*-orbital ordering in the Co^{2+} sublattice.

2.3 ELECTRICAL CONDUCTIVITY AND CHARGE - ORDERING

The experiments performed on polycrystalline samples showed antiferromagnetic (AF) insulating behaviour at low and high x values and ferromagnetic (F) metallic behaviour in a certain range of concentrations centred around $x \sim 1/3$. This striking behaviour was early explained by the theory of double – exchange DE [31, 32].

The transfer of e_g electron from Mn^{3+} to Mn^{4+} by DE is the basic mechanism of electrical conduction in the manganites. In those with strong DE, the e_g electrons become delocalized in the ferromagnetic phase for a certain range of doping centred around $x \sim 1/3$ and a FM state is established at low temperature. The conduction band of such a half-metallic ferromagnet is thus fully spin-polarized and is of large potential interest for spin electronics [48]. The electronic structure of $La_{1-x}M_xMnO_3$ (M = Ca, Sr, Ba) has been theoretically investigated by the local spin – density approximation (LSDA) [49, 50, 51]. The picture just outlined, of electronic hopping within narrow and fully spin – polarized bands is supportedby a band structure calculation made for the end members of one dilution series, $LaMnO_3$ and $CaMnO_3$ [52].

On the materials $RE(M)MnO_3$, the Hall effect in thin films $(La_{1-x}Gd_x)_{0.67}Ca_{0.33}MnO_3$ have been measured by Jaime *et al* [53] (Gd substitution is used here to lower $T_C \sim 130$ K). In the paramagnetic region the carrier sign is negative. This is argued to result from hopping processes involving odd-numbered Aharonov–Bohm loops, which means, for the perovskites, that next – nearest – neighbour hopping processes dominate charge transport.

Low-temperature transport – low-field magnetoresistance

The low-temperature transport can be divided into two distinct phenomena, the behaviour of the intrinsic, metallic or semiconducting, state which characterizes (sastoiania, koito harakterizirat) high-field MR, and that of the intergrain process which characterizes the low-field behaviour.

High – temperature resistivity

At high temperature, $T > T_C$ in the concentration region where CMR is strongest, $0.2 < x < 0.4$, transport is characterized by an activated resistivity, The discrepancy between these two temperatures was ascribed (by the authors) to the quasi – 2D nature of the Mn – O layers. The MR for this compound is much larger than for the 3D ($n = \infty$) system which illustrates the general trend of increasing MR with decreasing T_C.

The manganites with $x < 0.5$ have a conduction band more than half – filled whereas those with $x > 0.5$ have a conduction band less than half – filled and thus, the respective charge carriers are holes and electrons. They are currently labelled as hole-doped and electron-doped manganites, respectively. When increasing x above 0.5, the number of ferromagnetic DE links decreases and that of AF coupled Mn^{4+} increases. This favours AF or canted AF phases in which the motion of charge carriers is hindered.

Mixed-valence manganese oxides exhibiting a metal insulator transition accompanied by so – called colossal magnetoresistance (CMR) effects.

Table 1. Materials with manganese

Manganese oxides of general formula :
$RE_{1-x}M_xMnO_3$ (RE = rare – earth, M = Ca, Sr, Ba, Pb) – three – dimensional perovskite – type structure
(electronic structure : theoretically investigated by the local spin – density approximation (LSDA))
$La_{1-x}M_xMnO_3$ (M= Ca, Sr, Ba) – mixed – valence perovskites
$LaMnO_3$ – is the parent compound of the most investigated manganites for potential application by partial substitution of La by Ca and Sr.
$RE_{1-x}M_xMnO_3$: (RE- Gd, M- Pb,); (Mn, Te $\rightarrow$ O) – cubic perovskite structure
$La_{1-x}Ca_xMnO_3$
$La_{1-x}Sr_xMnO_3$: $La_{0.7}Sr_{0.3}MnO_3$

Manganite perovskites $T_{1-x}D_xMnO_3$ (where T is a trivalent lanthanide cation (e.g. La) and D is a divalent,. alkaline – earth cation (e.g. Ca, Sr, Ba):

For the end members of the dilution series, $LaMnO_3$ and $CaMnO_3$, the ground state is antiferromagnetic (AF), as expected for spins interacting via the superexchange interaction when the metal–oxygen–metal bond angle is close to 180°

$La_{0.67}Ca_{0.33}MnO_3$	thin film
$(La_{1-x}Gd_x)_{0.67}Ca_{0.33}MnO_3$	thin films (Gd substitution is used here to lower T_C ~ 130 K)

Disordered structure of the complex perovskite $Pb(Fe_{0.5}Ta_{0.5})O_3$:
$PbFe_{0.5}Ta_{0.5}O_3$ (PFT) - complex perovskite (first prepared as a ceramic).
This compound belongs to the wide family of lead – based oxides with general formula $PbB'_{0.5}B''_{0.5}O_3$, in which two cationic species, in a 1:1 ratio, occupy the B – site lattice of the perovskite structure ABO_3. These materials have been and still are extensively studied for their interesting ferroic behaviour.

Magnetic ordering in perovskites containing manganese and cobalt:

$RE(Mn_{1-x}Co_x)O_3$	(RE = Eu, Gd, Tb, Y)	
$EuMnO_3$ and $GdMnO_3$	– weak ferromagnets of Dzialoshinsky – Moriya type	
$TbMnO_3$		
$RE(Mn_{0.5}Co_{0.5})O_3$	(RE = Gd, Tb, Y).	the metamagnetic behaviour is interpreted taking into account the ionic ordering of Co^{2+} and Mn^{4+} ions
$La(Mn_{0.5}Me_{0.5})O_3$	(Me = Ni, Co) [1]	ternary oxides with a cubic perovskite structure are ferromagnets
$RE(Mn_{0.5}Co_{0.5})O_3$	(RE = Nd, Sm, Eu, Gd, Tb, Dy, Y)	these compounds – ferromagnets)
$RE(Mn_{1-x}Co_x)O_3$	(RE= Eu, Gd, Tb) perovskites	– containing manganese and cobalt ions

$GdMnO_{2.99}$
$GdFeO_3$ perovskite (in the Gd – ordered phase)
External magnetic field induces the antiferromagnet – ferromagnet transition for the Gd subsystem

SmSc materials with Mn and RE: In the case of the doped $A^{IV}B^{VI}$ semimagnetic semiconductors (SMSC) (example: $Pb_{1-x}Mn_XTe$, $Pb_{1-x}Gd_xTe$) was looked, after hot annealing on air (at temperature over 650 K) change of some properties- similar of the $RE(M=)MnO_3$ materials and some ceramics (structure perovskite, resistivity-CMR). The results are reported here.
PbMnTe – PbGdTe – PbSnMnTe – PbGdMnTe (Te ⇔ O)

---

3. SEMIMAGNETIC SEMICONDUCTORS

Manipulation of the spin degree of freedom in semiconductors has become a focus of interest in recent years. In the context of spin electronics, particularly interesting are ferromagnetic and semimagnetic (diluted magnetic) semiconductors (SMSCs). Understanding of the carrier-mediated ferromagnetism was initiated by a study of ferromagnetism in IV-VI based SMSCs. In this class of materials, deviations from stoichiometry result in the carrier density sufficiently high to produce strong ferromagnetic interactions between the localized spins. For example, it was shown that in $Pb_{1-x-y}Mn_xSn_yTe$ mixed crystals with high Sn concentration, $y \geq 0.6$, the free hole concentration can be varied by means of isothermal annealing in the range between 10^{20} and 10^{21} cm^{-3}. The alloys of IV – VI semiconductors and MnTe are a group of semimagnetic materials with very interesting magnetic properties. Ferromagnetic ordering was observed in $Sn_{1-x}Mn_xTe$ and in $Ge_{1-x}Mn_xTe$ [54] for $x >$

0.005. The freezing temperature is associated with the occurrence of a spin-glass state rather than a clustering effect. This result is attribute to the existence of long-range interband exchange interactions arising from the fact that $Pb_{1-x}Mn_xTe$ is a small-gap semiconductor. Above T_g, the material is in a superparamagnetic state due to short – range antiferromagnetic superexchange interactions.

Usually, transport properties (Hall – effect and resistivity as a function of temperature and the magnetic field) of magnetic semiconductors are not as spectacular as the magnetic properties. The impurity resistivity [55](78) [7] in spin-glasses varies roughly linearly with temperature around the freezing temperature T_g,, and then shows a broad maximum at a temperature T_m much larger than T_g. However, the application of an external magnetic field is expected to significantly modify the spin correlations. Consequently, the localized spins contribute significantly to the magnetic resistance (or to CMR for RE (M) MnO_3).

$Pb_{1-x}Mn_xTe$ is not a canonical spin-glass. This result is associated with the fact that the ferromagnetic coupling induced by the external magnetic field competes with the antiferromagnetic superexchange interactions which are shown to dominate at all the Mn concentrations investigated.

Other SmSc, (all known Eu-based IV – VI semimagnetic lead chalcogenides), with electrons as well as hole density below 10^{19} cm^{-3} are paramagnetic down to the temperature $T = 1$ K (similarly to Mn-based compounds). A strongly localized character of 4f orbitals of rare earth ions results in very weak exchange interactions both: 1 – between the magnetic ions, and 2 – between ions and the free carriers. As a result, the $Sn_{1-z}Eu_zTe$ crystals are not ferromagnetic. The reason for a lack of ferromagnetism in this material is the very small magnitude of the sp-f exchange integral. It has been known for several years that the Eu-Eu exchange interaction in these IV – VI SMSCs is two orders of magnitude smaller than the Mn-Mn exchange interaction in the traditional IV – VI SMSCs. The Mn-based IV–VI semimagnetic semiconductors with relatively low concentration of free carriers, for instance PbMnTe, are paramagnets above $T = 1$ K. Their magnetic behaviour closely resembles that of the Mn containing II–VI SMSCs and can also be attributed to antiferromagnetic interactions of the superexchange type, although the interactions are much weaker than in II-VI semimagnetic semiconductors. In this paper, we explore the influence of the presence of two types of magnetic ions, Mn^{2+} and Eu^{2+}, in the semiconductor matrix on the magnetic properties of resultant SMSC.

In this study has been a great deal of interest in a group of compounds de-

scribed as Semimagnetic semiconductors. The majority of these studies have been on chalcogenides of lead, tin, or cadmium containing manganese as the magnetic species. In the present paper, is considered the effect of the presence of two types of magnetic ions incorporated into semiconductor matrix on magnetic properties of the resultant semimagnetic semiconductor. In order to simplify the theoretical description of the investigated magnetic system, two types of magnetic ions were chosen with spin-only ground state: substitutional Mn^{2+} possesses $S = 5/2$. There are several reasons for which the magnetic semiconductors based on lead chalcogenides are ideal materials for such kind of investigations. First, a variety of magnetic properties has been observed in Mn-based IV-VI SMSCs. Second, the characteristic features are semi-metallic electric properties with well-developed methods of control of carrier concentration. At other materials as PbSn(RE)MnTe (for example $Pb_{1-x-y-z}Mn_xSn_yEu_zTe$) are a unique system in which the interplay between magnetic and electronic properties can be observed and studied. In particular, carrier-induced paramagnet-ferromagnet as well as ferromagnet-spin glass transitions have been observed. This is due to the combination of an RKKY type of interaction between the magnetic ions with the possibility of manipulating the free carrier concentration. These two features give IV-VI semimagnetic materials a distinguished position within the whole family of semimagnetic semiconductors. The additional advantage is that for the $Pb_{1-x-y}Mn_xSn_yTe$ crystals, the parameters of the energy structure are very well known.

Sample preparation and characterization

The crystals of SmSc were grown by a Bridgman method. In the present work, samples coming from several technological processes were investigated. Electron microprobe analysis (EDAX system at SEM) revealed good homogeneity of both the manganese and tin atom distributions in the samples. No second-phase inclusions were observed in X-ray measurements. Carrier concentrations (for SmSc alloys with Sn) were increased or decreased by thermal annealing in Te-rich or Sn-rich atmospheres, respectively.

The chemical composition of the samples was determined by the x-ray dispersive fluorescence analysis technique with uncertainty of 10%. Typically, the crystals were cut crosswise the growth axis to 1–2 mm thick slices. The variation of chemical composition along this area is very small (1–2%).

The standard powder x-ray measurements revealed that the investigated samples (PbMnTe, PbGdTe,PbMnSnTe, PbGdMnTe) are single-phase and crystallize in a NaCl structure, similarly to the nonmagnetic matrix and $Pb_{1-x-y}Mn_xSn_yTe$ semimagnetic semiconductor.. The introduction of Mn

ions into the nonmagnetic matrix of $Pb_{1-x}Sn_xTe$ leads to a decrease in the lattice constant of the resultant $Pb_{1-x-y}Mn_xSn_yTe$. All the investigated samples were characterized by means of low magnetic field transport measurements. The aim of the transport characterization was to obtain information about the elementary electric properties of the investigated samples: 1 – the type, and 2 – density of free carriers, and 3 – their mobility. In the case of IV–VI semimagnetic semiconductors, the carrier concentration is an important parameter since the change of the concentration influences the magnetic behaviour of the material. The transport experiments show that the valence band is significantly perturbed upon introduction of Mn in the matrix.

Magnetic Properties

Generally, in the range of high temperatures all IV – VI semimagnetic semiconductors (SmSc) are Curie-Weiss paramagnets with the temperature dependence of the magnetic susceptibility described by the Curie-Weiss law,

$$\chi(T) = \frac{C}{T - \Theta}, \tag{4}$$

where $C = g^2\mu^2_B S(S+1)N_M$ is the Curie constant and

$$\Theta = (1/3)S(S+1)x\sum z_i I(R_i)$$

is the paramagnetic Curie temperature (Curie-Weiss temperature).

For all the investigated samples the high temperature behaviour of the inverse low-field susceptibility χ^{-1} was nearly linear and all data fit well to the Curie-Weiss law of the form:

$$\chi(T) = \frac{C}{T - \Theta} + \chi_{dia}, \tag{5}$$

where χ_{dia} is the susceptibility of the host lattice (all IV-VI semiconductors without magnetic ions are standard diamagnetic materials with the magnetic susceptibility around $\chi_{dia} \cong 3 \times 10^{-7}$ emu g^{-1}).

A more pronounced influence of carrier concentration on the magnetic properties has been observed in [56] the magnetic semiconductors $Eu_{1-x}Gd_xSe$ and $Eu_{1-x}Gd_xTe$. The values of the paremagnetic Curie temperatures of these magnetic alloys are strongly gadolinium – content dependent. This effect is interpreted as the influence of electron – concentration via Ruderman–Kittel–Kasuya–Yosida–(RKKY) interaction (carriers are generated as a result of $Gd^{3+} – Eu^{2+}$ substitution).

PbSnMnTe is thus the first semimagnetic semiconductor material in which

the effect of the free – carrier concentration on the magnetic properties can be studied. The base compounds PbTe and SnTe are diamagnets.

It is clear from our experiments that the mechanism responsible for manganese – ion coupling in PbSnMnTe is carrier – concentration sensitive and long ranged (average interspin distance in the alloy $Pb_{1-x-y}Mn_xSn_yTe$ with $y = 0.03$ is approximately = 13 Å**).**

Among known exchange mechanisms only indirect exchange via carriers (RKKY interaction) seems to be sufficiently long ranged and effective in the high – carrier – concentration samples to account for the ferromagnetism of PbSnMnTe.

The $[((PbTe)_{1-x}(SnTe)_x]_{1-y}[MnTe]_y$ alloy, like $Sn_{1-x}Mn_xTe$ and $Pb_{1-x}Mn_xTe$, is a substitutional solid solution in which magnetic ions are randomly distributed in a metal *fcc* sublattice of the rock – salt crystal lattice. (as of that of PbTe). Materials can be grown with arbitrary tin content and with a wide range of manganese concentration (probably up to 15–20 at.%). Isothermal annealing in an appropriate atmosphere controls the number of metal vacancies and thereby the number of conducting holes. These technological properties of PbSnMnTe allow (or PbGdMnTe where Sn ↔ Gd) one to obtain samples with desired magnetic ion and tin concentrations, with the possibility of changing the carrier concentration in each sample over more than 1 order of magnitude. The Hall-effect was measured in the temperature region 77–300 K. According to Hall-effect measurements the hole concentration is constant bellow $T = 120$ K and monotonically decreases at higher temperatures [57].

Low-temperature ferromagnetism of dilute magnetic alloys is a well – known phenomenon in metallic alloys of transition metals. So – called giant moments are offen observed in such ferromagnets. Giant-moment formation does not take place in PbSnMnTe or other IV–VI – MnTe alloys because of diamagnetism of the host crystal.

According to the theory of dilute metallic alloys the magnetic – ion concentration practically determines the magnetic properties of the alloy. A similar situation is observed in dilute semiconducting magnetic alloys. In PbSnMnTe the situation is quite different. The magnetic properties are determined by both the magnetic–ion concentration and by charge – carrier concentration, and the magnetic-phase diagram includes carrier concentration as a parameter.

In conclusion we want to emphasize the extreme sensitivity of the magnetic properties of PbSnMnTe alloys to carrier concentration, and the unique possibility of generating ferromagnetic ordering by changes in the hole concentration alone. In these materials, the presence of substitutional Mn^{2+} ions carrying a bare spin of 5/2 is responsible for the magnetic properties [58–62].

In some of these papers were investigate the magnetic effects of introdusing Gadolinium into the semiconductor PbTe, and are compare these results with the earlier work on manganese in the same host. Gadolinium – doped PbTe and SnTe semiconductors have been studied in [23–28]. These systems are examples of narrow – gap dilute magnetic semiconductors. The interest in this class of compounds centres on the effect caused by the interactions between the carriers and the magnetic moment of the dopands. While the 3d dopand Mn has been extensively studied, less is known about the 4f dopand Gd. For Gd in PbTe and SnTe, Shubnikov–de Haas oscillations, as well as very high mobilities, are reported in [23]. The Curie–Weiss temperature θ in these alloys is small and negative, reflecting a weak antiferromagnetic exchange interaction between the Gd ions, similar to that of Mn in PbTe [29]. The materials$Pb_{1-x}Gd_xTe$ crystals were grown by the standart Bridgman technique (as described in [25]).

The measurements of electron paramagnetic resonance (EPR) and of susceptibility have been performed on $Pb_{0.995}Gd_{0.005}Te$ crystals. The Currie–Weiss temperature is negative and small for both clustered and single spins, reflecting a weak antiferromagnetic interaction.

The EPR spectra consist of two components, one showing the fine structure of Gd^{3+} ions in a cubic environment and the other a broad line, which is attributed to clusters of interacting Gd ions. An exchange-narrowing mechanism is responsible for the cluster line.

Both EPR and ac susceptibility results (above 10 K) show behaviour appropriate to a Gd S-state ion of spin 7/2 in the host PbTe matrix. The exchange interaction between Gd^{3+} ions is antiferromagnetic and weak.

This behaviour is similar to that reported for the S-state Mn^{2+} ions with spin 5/2 in the PbTe host. The decrease in paramagnetic susceptibility can be explained by model that allows for an antiferromagnetic clustering of impurity spins. In this model, if one assumes clusters formed by pairs of spins coupled antiferromagnetically, then the susceptibility results can be used to give an estimate of the number of spins that have formed clusters.

In some early investigations, from magnetic measurements (χ_o, EPR) decrease in paramagnetic susceptibility can be explained by a model that allows for antiferromagneting clustering of impurity spins.

The exchange interaction between Gd^{3+} ions is antiferromagnetic and weak. If the clusters formed by pairs of spins coupled antiferromagnetically, then the susceptibility results can be used to give an estimate of the number of spins that have formed clusters.

The Gd is trivalent while the Pb is divalent. Only part of the Gd ions

would be involved in interactions with the carriers, as would be required by the coexistence of the two spectra, then the model of interacting pairs or larger groups of Gd ions, i.e., clusters. For the lower concentrations, the EPR results indicate a fully resolved fine structure appropriate to the Gd^{3+} ion.

An inhomogeous distribution of Gd-ions in metallurgical or chemical clusters is not excluded by the above observations, but it is not the major source of the cluster signal. Below 100 K, the observed ratio of cluster-line intensity to single-ion intensity exceeds 20 :1.This discrepancy indicates that either the Gd ions are not randomly distributed or the interactions between them extend appreciably beyond nearest neighbours. When Gd is substituted for Pb in PbTe in the NaCl structure, it is surrounded by 12 cation sites connected to it by a pair of bonds at right angles. In addition, six more cation sites are connected by a pair of collinear bonds.

Three methods have been used for the "metallurgical" characterization of the samples: scanning electron microscopy (SEM), electron microprobe measurements and X-ray diffraction experiments. Only a single phase is visible in crystals with $x_n < 0.1$, from SEM observations, even at high magnification (8000 X). It is worth noticing that a good radial homogeneity and reproducible values are found from electron – microprobe measurements in samples with $x_n = 0.15$ (and 0.20). This discrepancy with the SEM observation is likely to be due to the diffusion volume of the electron beam, which is very important as is its impact area.

The variations of Mn composition, as determined by electron – microprobe analysis, is reported as a function of the distance *d* from from the bottom of the ingots along the axis in (Fig.8) and (Fig.9) The normal freezing in the case of partial mixing in non – volatile liquids is expressed by the law:

$$x_n(d) = \mathrm{k}c_o(1 - d/\mathrm{l})^{\mathrm{k}-1}, \tag{6}$$

here, x_n is the concentration of manganese in the ingot, k is the interface distribution coefficient, c_o is the initial value of the uniform concentration of solute in the liquid, and l is the total length of the ingot.

For $x_n \sim 0.03$ and $x_n \sim 0.1$, the experimental data can actually be fitted by Eq.7 (Fig.8). This confirms the solid – solution character of alloys of composition ranging up to $x_n \sim 0.1$. The alloys have also been studied by X-ray diffraction. Lead telluride has a cubic NaCL structure with a lattice parameter, measured in our samples, equal to 6.46 Å, in agreement with previous results. Alloys up to $x_n = 0.1$ keep the same structure, and their parameters seem to follow Vegard's law, as shown in (Fig.10). On the contrary, crystals with $x_n \sim 0.15$ present additional lines corresponding to hexagonal MnTe. The lines associ-

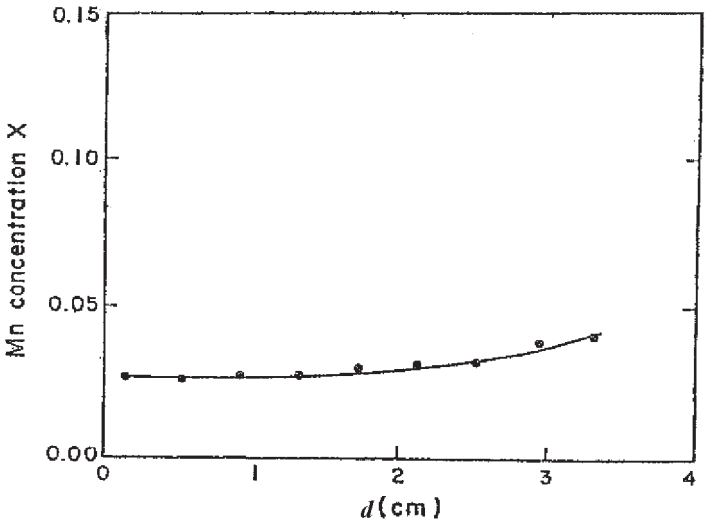

Fig.8. Manganese concentration x in $Pb_{1-x}Mn_xTe$ as a function of the distance d from the extremity of the ingot for low Mn-concentrations.

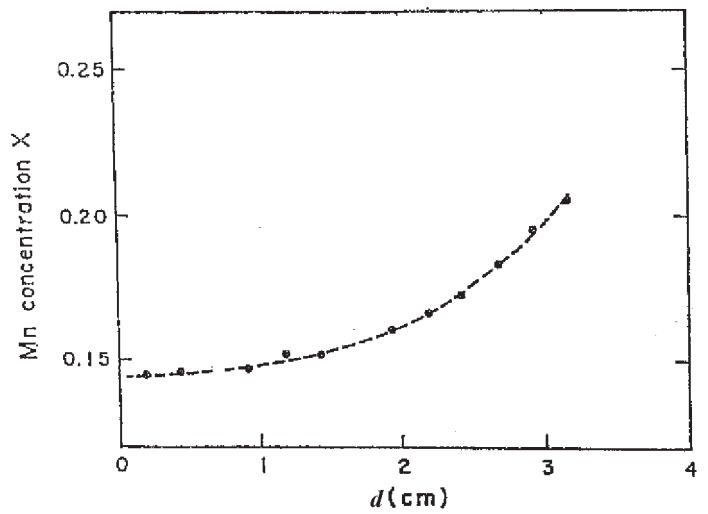

Fig.9. Manganese concentration x in $Pb_{1-x}Mn_xTe$ as a function of the distance d from the extremity of the ingot for larger Mn-concentrations. (The dashed curve is guide for the eyes only)

ated with PbTe are split in triplets, indicating a deformation of the cubic NaCl structure towards an hexagonal structure. The lattice parameters determined for the cubic PbTe-rich phase present in the $x_n = 0.15$ correspond to alloys of

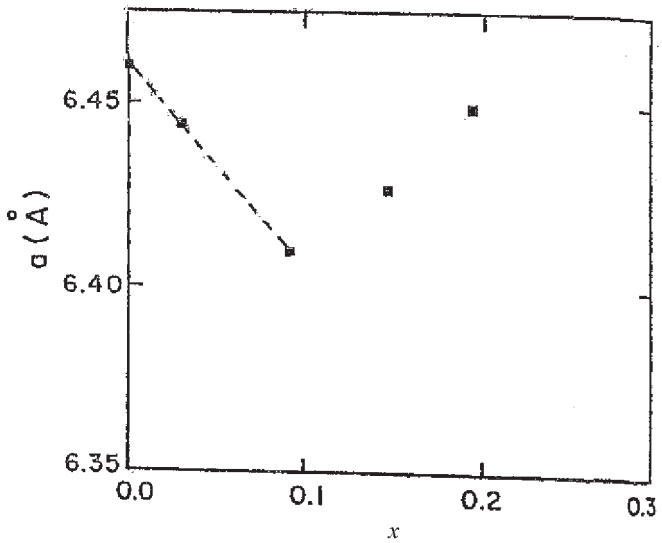

Fig.10. Variations of the lattice parameter *a* as a function of the Mn-concentration *x* in $Pb_{1-x}Mn_xTe$

lower Mn concentrations. However, homogeneous $Pb_{1-x}Mn_xTe$ has been prepared up to $x_n = 0.115$ by Bridgman method (as described in [63]).

In the limit of small Mn concentrations, only two configurations of Mn ions have a significative probability to occur in a statistical distribution, namely single ions and pairs. Since the pairs are antiferromagnetically coupled by the strong superexchange interaction, only the Mn ions which contribute to the magnetic properties in the range of temperature investigated are single ions. In the fcc lattice each atom has 12 first neighbors.

Electronic Structure

This feature may be ascribed to the Gd-sublattice contribution. Apparently the $f - d$ exchange interaction modifies the magnetic state of the 3*d* sublattice. The negative value of residual magnetization at low temperature arises from Gd magnetic moment ordering. Such a behaviour indicates the negative total $f - d$ superexchange and large magnetic anisotropy. The magnetic moment of Gd ions is opposite to the total magnetic moment of the 3*d* sublattice. The compositions with $0.4 < x < 0.7$ exhibit sharp transitions into the paramagnetic state.

In conclusion, here have investigated the quarternary materials PbGdMnTe with values of rare -earth ion concentrations x up to $x = 0.02$. The values of (x) and magnetic ion concentration were chosen to keep the energi gap constant

and approximately equal to that value of host crystal PbTe. These crystals are n–type conductivity with carrier concentrations ranging from $8x10^{18}$ to 10^{19} cm^{-3}. The concentration of the magnetic ions in investigated single crystals were determined by electron-microprobe and lattice parameters were estimated by X-ray measurements with an accuracy of about 20 %. There was less than a 5% variation in magnetic ion concentration throughout each sample.

Single crystals of IV–VI chalcogenides containing Mn and rare – earth ions, substitutionally replacing ione of the cations, have been grown by the Bridgman technique. Measurements have shown the strong influence of a magnetic field on the physical properties of these diluted – magnetic semiconducting materials.

Previously were measured the high – temperature mobility and conductivity of the ternary alloys $Pb_{1-x}Mn_xTe$ and $Pb_{1-x}Gd_xTe$ and compared these values with values of the samples with the same compositions which were annealed in air. The magnitude of the resistivity of annealed samples were found to be significantly larger, than the resistivity on other none annealed materials. These results are consistent with a model based on formation of manganese oxides, in sequence of change of Te ions by oxide. In the case of annealing on air of the samples PbGdMnTe, mechanical investigations shown increase of microhardness. It is possible formation of phase perovskite type in annealed samples.

The crystal lattice (unit-cell parameter) of host material PbTe is extremaly sensitive to the change of concentration, and to the cation–anion separation: or to the substitude of oxide ions to telluride and formation of MnO phase in the samles. These preliminary results have been needed from other structural investigations, as X-ray diffraction measurements.

SUMMARY

In this paper, the results of structural, magnetic and transport studies of RE(M)MnO_3 materials, ceramics and SmSc multinary alloys are reported. The following results were obtained. At materials metal–insulator, ceramics and semimagnetic semiconductors are observed similar properties and phenomena as: (i) transitions: ferro-paramagnetic and antiferro–ferromagnetic (exchange and superexchage) interactions (external magnetic field induces the antiferromagnet–ferromagnet transition for the Gd subsystem; such a transition has been observed for Gd-FeO_3 perovskite in the Gd ordered phase); (ii) Valided dependence T_c from RE concentration; (iii) transitions of structure (rock salt to perovskite by oxide atom substitution to Te).

Colossal magnetoresistance in the manganite perovskites is only one facet of a complex many – body phenomenon. The combined metal – insulator and ferro – paramagnetic transition and its description in terms of a double – exchange interaction provide the starting point for a microscopic description of the various ground states.

In the case of Pb(RE=Gd,Eu)MnTe crystals, the obtained negative and relatively small

values of the paramagnetic Curie–Weiss temperature Θ indicate that a weak antiferromagnetic superexchange interaction is a dominant mechanism of the interaction. These results correspond to those reported earlier for PbMnTe.

The presence of two types of magnetic ions (Mn and Eu) in the IV – VI semiconductor matrix influences the magnetic properties of the resultant magnetic semiconductor. The results of magnetic measurements show that the Curie temperature T_C as well as the Curie-Weiss temperature Θ decrease with an increase of the rare earth element content in samples.

The qualitative analysis shows that a variation of the band parameters with the alloy composition can be responsible for the observed strong dependence of the Curie temperature on the RE content. A simple two-band model explains both the order of the transition temperature values and T_C dependence on RE concentration. The dependence of the Curie temperature on the rare – earth (Eu or Gd) content clearly demonstrates that the magnetism of semiconductors can be effectively controlled by using an energy band structure dependence on alloy composition. The situation with several non-equivalent energy minima is not unique for IV-VI semiconductors. It can be used to increase the critical temperature of ferromagnetism in magnetically-doped semiconductors.

In the case of the doped $A^{IV}B^{VI}$ semimagnetic semiconductors (SMSC) (example: $Pb_{1-x}Mn_XTe$, $Pb_{1-x}Gd_xTe$) ware looked, after hot annealing on air (at temperature over 450 K) change of some properties — similar of the RE(M=)MnO_3 materials and some ceramics (structure– perovskite, resistivity- CMR). It is possible that SmSc shows the temperature – induced transition from rock-salt (collinear) to perovskite (spiral magnetic) structure. associated with oxide atoms ordering in the Te sublattice. Such a transition could observed for PbMnTe and PbGdTe NaCl in the GdTe and MnTe – ordered phase. Or of the case of rare-earth SmSc with MnTe phase this phenomenon can observed at relatively high temperatures.

REFERENCES

1. Morimoto, I., A. Asamitsu, H. Kuwahara, Y. Tokura. *Nature*, **380**, 1996, 141.
2. Kobayashi, K.I., T. Kimura, H. Sawad, K. Terakura, Y. Tokura. *Nature*, **395**, 1998, 677.
3. Hase, M., I. Terasaki, K. Uchinokura. *Phys. Rev. Lett.*, **70**, 1993, 3651.
4. Kusters, R.M., J. Singleton, D.A. Keen, R. McGreevy, W. Hayes. *Physica B*, **155**, 1989, 362.
5. Helmot von, R., J. Wecker, B. Holzapfel, L. Schultz, K. Samwer. *Phys. Rev. Lett.*, **71**, 1993, 2331.
6. Chahara, K., T.Ohno, M. Kasai, Y. Kozono. *Appl. Phys. Lett.*, **63**, 1993, 1990.
7. Jin, S., T.H. Tiefel, M. Mc Cormack, R.A. Fastnacht, R. Ramesh, L.H. Chen. *Science*, **264**, 1994, 413.
8. Ramirez, A.P. *J. Phys: Condens. Matter.*, **9**, 1997, 8171. review art.
9. Rao, C.N.R., A. Arulraj, A.K. Cheethan, B. Raveau. *J. Phys.: Condens. Matter.*, **12**, 2000, R83.
10. Zener, C. *Phys. Rev.*, **81**, 1951, 440.
11. Yunoki, S., J. Hu, A.L. Malvezzi, A. Moreo, N. Furukawa, E. Dagotto. *Phys. Rev. Lett.*, **80**, 1998, 845.
12. Nagaev, E.L. *Phys. Uspekhi*, **39**, 1996, 781.
13. Hennion, M., F. Moussa, J. Carvajal-Rodriguez, L. Pinsard, A. Revcolevschi. *Phys. Rev. B.*, **56**, 1997, R497.

14. Smolenscii, G.A., A.I. Agranovskaia, V.A. Ysupov. *Fiz. Tverd. Tela*, **1**, 1959, 990.
15. Goodenough, J.B., A. Wold, R.J. Arnott, K.N. Menyuk. *Phys. Rev.*, **124**, 1961, 373.
16. Blasse, G. *J. Phys. Chem. Solids*, **26**, 1965, 1969.
17. Sonobe, M., K. Asai. *J. Phys. Soc. Japan*, **61**, 1992, 4193.
18. Nishimori, N., K. Asai, M. Mizoguchi. *J.Phys. Soc. Japan*,**64**,1995, 1326.
19. Cohen, J., A. Globa, P. Mollard, M. Rodot. *J. Phys*. (Paris), **29**, 1968, 142.
20. Lewis, J.E., M. Rodot. *J. Phys*. (Paris) **29**, 1968, 352.
21. Toth, G., J.Y. Le Poup, M. Rodot. *Phys. Rev. B*, **1**, 1970, 4573.
22. Hamasaki, T. *Solid State Commun*. **32**, 1979, 1069.
23. Averous, M., B.A. Lombos, C. Fau, E. Ilbnouelchazi, J.C. Tedenac, G.Brun, M. Bartkowski. *Phys. Stat. Solidi B*, **131**, 1985, 759.
24. Hedgcock, F.T., P.C. Sullivan, M. Bartkowski. *Low Temperature Physics*, LT17 (Elsevier, Amsterdam. The Netherlands 1984) CQ13.
25. Hedgcock, F.T., P.C. Sullivan, J.T. Grembowiz, M. Bartko. *Can. J. Phys*. **64**, 1986, 1345
26. Bartkowski, M., D.J. Northcott, A.H. Redddoch. *SolidState Commun*. **56**, 1985, 659.
27. Savage, H.T., J.J. Rhyne. *AIP Conf. Proc*. **5**, 1971, 879.
28. Han, B.S., O.G. Symco, D.J. Zheng, F.T. Hedgcock. *Materials Research Society. Fall Meeting* (Boston, MA, 1986 Abstract) Q3.3.
29. Bartkowski, M., A.H. Reddoch, D.F. Williams, G. Lamarche, Z. Korczak. *Solid State Commun*. **57**, 1986, 185.
30. Wollan, E.O., W.C. Koehler. *Phys. Rev.*, **100**, 1955, 545.
31. Zener, C. *Phys. Rev.*, **81**, 1951, 440.
32. Goodenough, J.B., *Phys. Rev.*, **100**, 1955, 564.
33. De Gennes, P.G. *Phys. Rev.*, **118**, 1960, 141.
34. Millis, A.J., P.B. Littlewood, B.I. Shraiman. *Phys. Rev. Lett.*, **74**, 1995, 5144.
35. Jin, S., T.H. Tiefel, M. McCormack, R.A. Fastnacht, R. Ramesh, J.H. Chen. *Science*, **264**, 1994, 413.
36. Wollan, E.O., W.C. Koehler. *Phys. Rev.*, **100**, 1955, 545.
37. Ramirez, A.P., P. Schiffer, S.W. Cheong, W. Bao, T.T.M. Palstra, P.L. Gammel, D.J. Bishop, B. Zegarski. *Phys. Rev. Lett.*, **76**, 1996, 3188.
38. Shimakawa, Y., Y, Kubo, T. Manako. *Nature*, **379**, 1996, 53.
39. Elemans, J.B.A., B. Van Laar, K.R. Van der Veen, B.O. Loopstra. *J. Solid State Chem.*, **3**, 1971, 238.
40. Goodenough, J.B. *Phys. Rev.*, **100**, 1955, 564.
41. Coey, J.M.D., M. Virett, L.Ranno, K. Qunadjela. *Phys. Rev. Lett.*, **75**, 1995, 3910.
42. Hwang, H.Y., S.W. Cheong, P.G. Radaelli, M. Marezzio, B. Batlogg. *Phys. Rev. Lett.*, **75**, 1995, 914.
43. Damay, F., A. Maignan, C. Martin, B. Raveau. *J. Appl. Phys.*, **81**, 1997, 1372.
44. Anane, A., C. Dupas, K. LeDang, J.P. Renard, P. Veilett, L. Pinsard, A. Revcoleschi. *Appl. Phys. Lett.*, **69**, 1996, 1160.
45. Comes, R., M. Lambert, A. Guinier. *Acta Crystallogr.*, **A26**, 1970, 244.
46. de Nathan, N., E. Husson, G. Calvarin, J.R. Gavarri, A.W. Hewatt, A. Morewell. *J. Phys.: Condens. Matter.*, **3**, 1991, 8159.
47. Huang, Q., A. Santoro, J.W. Lynn, R.W. Erwin, J.A. Borchers, J.L. Peng, R.L. Green. *Phys. Rev. B*, **55**, 1997, 14987.
48. Greeg, J.F., I. Petej, E. Jouguelet, C. Dennis. *J. Phys. D: Appl. Phys.*, **35**, 2002, R121.
49. Sathpathy, A., Z.S. Popovic, F.R. Vukajlovic. *Phys. Rev. Lett.*, **76**, 1996, 960.

50. Pickett, W.E., D.J. Singh. *Phys. Rev. B*, **53**, 1996, 1146.
51. Singh, D.J., W.E. Pickett. *Phys. Rev. B*, **57**, 1998, 88.
52. Satpathy, S., Z.S. Popovic, F.R. Vukajlovic. *Phys. Rev. Lett.*, **76**, 1996, 960.
53. Jaime, M., H.T. Hardner, M.B. Salamon, M. Rubinstein, P. Dorsey, D. Emin. *Phys. Rev. Lett.*, **78**, 1997, 951.
54. Cochrane, R.W., M. Plischke, J.O. Strom – Olsen. *Phys. Rev. B*, **9**, 1974, 3013.
55. Mydosh, J.A., P.J. Ford, M.P. Kawatra, T.E. Whall. *Phys. Rev. B*, **10**, 1974, 2845.
56. Holtzberg, F., T.R. McGuirem, S. Methfessel, J.C. Suits. *Phys. Rev. Lett.*, **13**, 1964, 18.
57. Story, T., A. Lewicki, A. Szczerbakow. *Acta Phys. Pol*. **A67**, 1985, 317.
58. Cochrane., R.W., M. Plischke, J. Strom – Olsen. *Phys. Rev. B*, **9**, 1973, 3031.
59. Gaz,J.A., R.R.Galazka, M.Nawrochi. *Solid State Commun*. **23**, 1977, 894.
60. Tanaka, K., M.Ishebone, M.Inoue, H.Yagi. *J. Appl. Phys*. **16**, 1977, 783.
61. Galazka, R.R., S. Nagato, P.N. Keesom. *Phys. Rev. B*, **22**, 1980, 3344.
62. Oseroff, S., F. Acker. *Solid State Commun*. **7**, 1980, 19.
63. Triboulet, R., G. Didier. *J. Cryst. Growth*, **52**, 1981, 614.

Received September 2007

Zahari Zlatanov
St. Kliment Ohridski University of Sofia
Faculty of Phisics
Department of General Phisics
5, James Bourchier Blvd
1164 Sofia, Bulgaria
E-mail: zlatanov@phys.uni-sofia.bg